Crystal Structure of Bis(4-methylimidazole)tetraphenylporphyrinatoiron(III) Chloride and Related Compounds. Correlation of Ground State with Fe−N Bond Lengths

Jack Silver,*,† Paul J. Marsh,† Martyn C. R. Symons,† Dimitri A. Svistunenko,‡ Christopher S. Frampton,*,§ and George R. Fern†

School of Chemical and Life Sciences, Woolwich Campus, University of Greenwich, Wellington Street, Woolwich, London, SE18 6PF, U.K., Department of Biological Sciences, Central Campus, University of Essex, Wivenhoe Park, Colchester, Essex, C04 3SQ, U.K., and Roche, Discovery Welwyn, Broadwater Road, Welwyn Garden City, Hertfordshire, AL7 2AY, U.K.

Received July 16, 1999

The crystal structure of the title compound is presented and shown to be one of a class of low-spin iron porphyrin complexes having a ground-state electronic configuration of $(d_{xy})^2(d_{xz})^2(d_{yz})^1$. If their Fe−N bond lengths (average N-porphyrin plotted against average N-axial) are considered, this class of low-spin iron(III) porphyrins of general formula $[Fe^{III}Por(L)_2]^+X^-$ and of ^2B ground state is shown to be distinctly different crystallographically from a similar class of compounds with the same general formula but with a ^2E or a $(d_{xy})^2(d_{xz},d_{yz})^3$ ground state. A third group of compounds with the same general formula have a $(d_{xz},d_{yz})^4(d_{xy})^1$ ground state and again are in a different region of the plot. Compounds showing intermediate properties can be forecast from the simple relationship presented in this work. The electron paramagenetic resonance data are shown to be dependent on the ground state, and those of configuration $(d_{xy})^2(d_{xz},d_{yz})^3$ and the ^2B ground state obey a correlation previously suggested in the literature.

Introduction

There have been a number of studies of bis-ligated porphyrinato iron(III) complexes, $[Fe^{III}Por(L)_2]^+$, where the axial ligands (L) are aliphatic amines,[1,2] histidine,[3] imidazole, or substituted imidazoles,[4−20] as models for cytochromes *b*. These model compounds have been extremely useful as aids to the understanding of the bonding and properties of the haems in such proteins.

It is well-known, from studies of cytochromes *b* from various mitochondrial and chloroplast sources, that the haem (iron protoporphyrin IX) in these proteins is coordinated to two histidine residues.[21−28] The principal mechanisms of fine control of haem iron reactivity in haemoproteins arise from the electronic and steric influences of these ubiquitous ligands.[29] Studies of the physical properties of the cytochrome *b* proteins have focused on the orientation of the imidazole planes of the axial histidine ligands.[8,15,18,24,30] Cytochromes *b* from complex III of mitochondria give electron paramagnetic resonance (EPR)

† University of Greenwich.
‡ University of Essex.
§ Roche, Discovery Welwyn.

(1) Marsh, P. J.; Silver, J.; Symons, M. C. R.; Taiwo, F. A. *J. Chem. Soc., Dalton Trans.* **1996**, 2361−2369.
(2) Marques, H. M.; Munro, O. Q.; Crawcour, M. L. *Inorg. Chim. Acta* **1992**, *96*, 221−229.
(3) Medhi, O. K.; Silver, J. *J. Chem. Soc., Dalton Trans.* **1990**, 555−559.
(4) Medhi, O. K.; Silver, J. *J. Chem. Soc., Dalton. Trans.* **1990**, 263−270.
(5) Scheidt, W. R.; Osvath, S. R.; Lee, Y. J. *J. Am. Chem. Soc.* **1987**, *109*, 1958−1963.
(6) Collins, D. M.; Countryman, R.; Hoard, J. L. *J. Am. Chem. Soc.* **1972**, *94*, 2066−2072.
(7) Hatano, K.; Safo, M. K.; Walker, F. A.; Scheidt, W. R. *Inorg. Chem.* **1991**, *30*, 1643−1650.
(8) Walker, F. A.; Huynh, B. H.; Scheidt, W. R.; Osvath, S. R. *J. Am. Chem. Soc.* **1986**, *108*, 5288−5297.
(9) Safo, M. K.; Gupta, G. P.; Walker, F. A.; Scheidt, W. R. *J. Am. Chem. Soc.* **1991**, *113*, 5497−5510.
(10) Yoshimura, T.; Ozaki, T. *Arch. Biochem. Biophys.* **1984**, *230*, 466−482.
(11) Higgins, T. B.; Safo, M. K.; Scheidt, W. R. *Inorg. Chim. Acta* **1990**, *178*, 261−267.
(12) Nakamura, M.; Tajima, K.; Tada, K.; Ishizu, K.; Nakamura, N. *Inorg. Chim. Acta* **1994**, *224*, 113−124.
(13) Quinn, R.; Valentine, J. S.; Byrn, M. P.; Strouse, C. E. *J. Am. Chem. Soc.* **1987**, *109*, 3301−3308.
(14) Quinn, R.; Strouse, C. E.; Valentine, J. S. *Inorg. Chem.* **1983**, *22*, 3934−3940.
(15) Walker, F. A.; Reis, D.; Balke, V. L. *J. Am. Chem. Soc.* **1984**, *106*, 6888−6898.
(16) Little, R. G.; Dymock, K. R.; Ibers, J. A. *J. Am. Chem. Soc.* **1975**, *97*, 4532−4539.
(17) Epstein, L. M.; Straub, D. K.; Marricondi, C. *Inorg. Chem.* **1967**, *6*, 1720−1724.
(18) Scheidt, W. R.; Chipman, D. M. *J. Am. Chem. Soc.* **1986**, *108*, 1163−1167.
(19) Soltis, S. M.; Strouse, C. E. *J. Am. Chem. Soc.* **1988**, *110*, 2824−2829.
(20) Scheidt, W. R.; Kirner, J. L.; Hoard, J. L.; Reed, C. A. *J. Am. Chem. Soc.* **1987**, *109*, 1963−1968.
(21) Matthews, F. S.; Czerwinski, E. W.; Argos, P. In *The Porphyrins*; Dolphin, D., Ed.; Academic Press: New York, 1979; Vol. 7, pp 108−147.
(22) Iyanagi, T. *Biochemistry* **1977**, *16*, 2725−2730.
(23) Widger, W. R.; Cramer, W. A.; Herrman, R. G.; Trebst, A. *Proc. Natl. Acad. Sci. U.S.A.* **1984**, *81*, 674−678.
(24) Babcock, G. T.; Widger, W. R.; Cramer, W. A.; Oertlings, W. A.; Mertz, J. *Biochemistry* **1985**, *24*, 3638−3645.
(25) Keller, R.; Groudinsky, O.; Wüthrich, K. *Biochim. Biophys. Acta* **1973**, *328*, 233−238.
(26) Blumberg, W. E.; Peisach, J. In *Cytochrome Oxidase*; King, T. E., Orii, Y., Chance, B., Okuniki, K., Eds.; Elsevier: Amsterdam, 1979; pp 153−159.
(27) Babcock, G. T.; Callahan, P. M.; Ondrias, M. R.; Salmeen, I. *Biochemistry* **1981**, *20*, 959−966.
(28) Moore, G. R.; Williams, R. J. P. *FEBS Lett.* **1977**, *79*, 229−232.
(29) Perutz, M. F.; Ten Eyck, L. F. *Cold Spring Harbor Symp. Quant. Biol.* **1971**, *36*, 295.

10.1021/ic990848s CCC: $19.00
Published on Web 06/02/2000

Table 1. X-band EPR Data for Compounds of the Type $[Fe^{III}Por(L)_2]^+X^-$ Where L = Imidazole or Subsituted Imidazole Presented in Order of Increasing g_z Values

no.[a]	complex[b]	temp (K)	g_z	g_y	g_x	ϕ (deg)	V/Δ	ref
7	$[K(K222)][Fe^{III}TPP(4\text{-}MeIm^-)_2]$	77	2.6	2.24	1.82	1/17	0.66	14
	$[Fe^{III}TPP(HIm)_2]Cl$[c]	77	2.67	2.33	1.84		0.76	this work
6	$[Fe^{III}TPP(4\text{-}MeIm)_2]Cl$ (crystalline)	110	2.86	2.3	1.59	4[d]	0.65	this work
	$[Fe^{III}TPP(4\text{-}MeIm)_2]Cl$ ($CHCl_3$)	100	2.85	2.29	1.59		0.64	15
9	$[Fe^{III}TPP(1\text{-}MeIm)_2]ClO_4$	77	2.87	2.28	1.54	22/32	0.64	11
8	$[Fe^{III}T2,6\text{-}Cl_2PP(1\text{-}VinIm)_2]ClO_4$	7	2.9	2.27	1.57	14/20	0.64	7
1	$[Fe^{III}TPP(HIm)_2]Cl$	86	2.92	2.31	1.55	5	0.64	19
	$[Fe^{III}TPP(HIm)_2]Cl$	77	2.95	2.33	1.57		0.63	this work
3	$[Fe^{III}TPP(t\text{-}MU)_2]SbF_6$	77	2.96	2.27	1.47	22	0.58	13
2	$[Fe^{III}TPP(c\text{-}MU)_2]SbF_6$	77	2.97	2.30	1.49	15	0.61	13
5	$[Fe^{III}TPP(HIm)_2]Cl$	86	2.99	2.27	1.48	41	0.57	19
4	$[Fe^{III}TPP(c\text{-}MU)_2]SbF_6$	77	3.00	2.27	1.48	29	0.55	13

[a] Figure 1. [b] K222 ≡ Kryptofix 222. PPIX ≡ protoporphyrinato IX dianion. T2,6-Cl_2PP ≡ 5,10,15,20-tetrakis(2,6-dichlorphenyl)porphyrinato dianion. [c] Site found in $[Fe^{III}TPP(Him)_2]Cl$ that is ascribed to the structure reported by Hoard et al.[6] [d] Average value of molecules **6a** and **6b**.

spectra[31−34] known as "large g_{max}". A "large g_{max}" spectrum consists of an intense g_z value at $g \geq 3.3$; the g_y and g_x values are often not seen at all in the spectrum. Complexes in which the imidazole planes on either side of the iron porphyrin plane are perpendicular to each other give rise to this type of spectrum.[9,15] The Mössbauer quadrupole splitting (ΔE_Q) values are around 1.8 mm s^{-1}.[4] Such perpendicular orientation of the imidazole ligands relative to each other is found for iron porphyrin complexes where the binding of the imidazoles is sterically hindered. Cytochrome b_5 proteins have rhombic EPR spectra with $g_z \approx 3.0$, $g_y \approx 2.2$, and $g_x \approx 1.4$.[35−38] These g values are in the range observed for model compounds[4−15] in which the imidazole planes are in parallel orientation. Complexes with ΔE_Q values of ∼2.25−2.4 mm s^{-1} have been assigned to this orientation.[4,17] The bis(histidine)protoporphyrinato(IX)iron(III) complex gave a ΔE_Q value of 2.14 mm s^{-1} and large line widths, which suggested that the histidines bind as sterically hindered imidazoles and that there was a large angle between the two imidazole planes.[3]

Hoard et al.[6] first used the symbol "ϕ" to describe the angle from the intersection of the plane of the axial ligand and the porphyrin plane to the nearest Fe−N_{por} vector. Strouse et al.[13,19] have reported a correlation of the crystal field parameter V/Δ with ϕ for five $[Fe^{III}TPP(L)_2]^+$ complexes (**1**−**5**) (TPP = 5,10,15,20-tetraphenylporphyrinato dianion, L = imidazole or substituted imidazole) with different ϕ values (Table 1, Figure 1). In this paper, we present an extended study of the effect of ϕ on crystal field parameters. This includes complexes **1**−**5** used in the studies by Strouse et al.[13,19] and, using both literature data[7,11,13,14,19] and new results, a further four $[Fe^{III}Por(L)_2]^+$ complexes (**6**−**9**) (Table 1, Figure 1). We also report the crystal and molecular structure of $[Fe^{III}TPP(4\text{-}MeIm)_2]Cl$ (**6**), and by comparing this structure with those of other known low-spin complexes, we show a simple relationship between their structures and the ground-state electronic configuration.

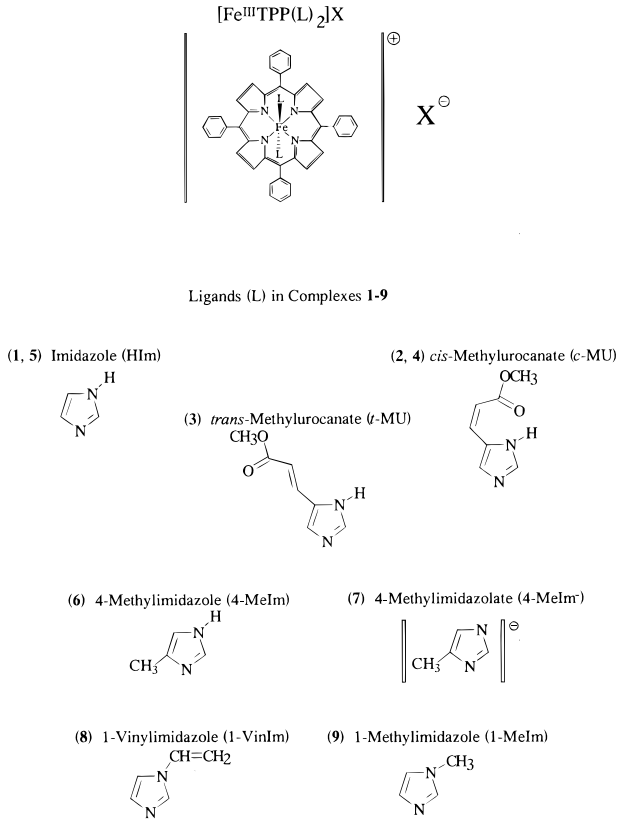

Figure 1. Ligands in $[Fe^{III}TPP(L)_2]X$ complexes **1**−**9**.

Experimental Section

Materials. Imidazole and 4-methylimidazole were purchased from Aldrich Chemical Co., and chloroform and hexane were from Fisher Scientific, U.K. All chemicals were used without further purification.

a. Preparation of Bis(imidazole)tetraphenylporphyrinatoiron(III). The complexes were prepared using the method of Scheidt et al.[5] as follows. $[Fe^{III}TPP(Cl)]$ (0.07 g; 0.1 mmol) and imidazole (0.04 g; 0.6 mmol) were dissolved in chloroform (4 mL). A 1:2 chloroform/hexane mixture (9 mL) was allowed to diffuse into the solution. Very small single crystals were obtained after 1−2 days. Anal. Calcd for $[Fe^{III}TPP(Him)_2]Cl{\cdot}CHCl_3{\cdot}H_2O$: C, 62.81; H, 3.99; N, 11.49. Found: C, 62.44; H, 3.93; N, 11.66. Crystal data: $a = 11.064(2)$ Å, $b = 13.147(2)$ Å, $c = 17.648(4)$ Å, $\alpha = 70.01(1)°$, $\beta = 72.52(2)°$, $\gamma = 86.29(1)°$, $V = 2298.8(8)$ Å^3. The cell is identical with that published by Scheidt et al.[5] Our cell is slightly smaller because it was collected at 123 K. This shows that the sample contained material of the same structure as that reported by Scheidt et al.[5] However, as will be seen in the following text, this material was prepared several times. The analysis was always similar to that given above, but in one sample a second form must have been present (see Results and Discussion).

(30) Carter, K. R.; Tsai, A.; Palmer, G. *FEBS Lett.* **1981**, *132*, 243−246.
(31) Tsai, A.-L.; Palmer, G. *Biochim. Biophys. Acta* **1983**, *722*, 349−363.
(32) Salerno, J. C.; McGill, J. W.; Gerstile, G. C. *FEBS Lett.* **1983**, *162*, 257−261.
(33) Leigh, J. S.; Erecinska, M. *Biochim. Biophys. Acta* **1975**, *387*, 95−106.
(34) Erecinska, M.; Oshino, R.; Oshino, N.; Chance, B. *Arch. Biochem. Biophys.* **1973**, *157*, 431−445.
(35) Rivera, M.; Barillas-Mury, C.; Christensen, K. A.; Little, J. W.; Wells, M. A.; Walker, F. A. *Biochemistry* **1992**, *31*, 12233−12240.
(36) Von Bodman, S. B.; Schuler, M. A.; Jollie, D. R.; Sligar, S. G. *Proc. Natl. Acad. Sci. U.S.A.* **1986**, *83*, 9443−9447.
(37) Ikeda, M.; Izuka, T.; Takao, H.; Hagihara, B. *Biochim. Biophys. Acta* **1974**, *336*, 15−24.
(38) Passon, P. G.; Reed, D. W.; Hultquist, D. E. *Biochim. Biophys. Acta* **1972**, *275*, 51−61.

Table 2. Mössbauer Data for Compounds of the Type $[Fe^{III}Por(L)_2]^+X^-$ Where L = Imidazole Type Ligand (Values Recorded at ~77 K Unless Otherwise Stated)

no.	compound	solvent	δ (mms^{-1})[a]	ΔE_Q (mm s^{-1})	Γ (mm s^{-1})[b]	ref
	$[Fe^{III}TPP(HIm)_2]Cl$	crystalline	0.28(2)	2.22(2)	0.33(2)/0.46(3)	this work
	$[Fe^{III}TPP(HIm)_2]Cl$	solid	0.50	2.23	not given	17
	$[Fe^{III}TPP(HIm)_2]Cl$ (room temp)	solid	0.40	2.11	not given	17
	$[Fe^{III}TPP(HIm)_2]Cl$[c]	solid	0.25(1)	2.09(1)	0.29(1)/0.45(1)	this work
	$[Fe^{III}TPP(HIm)_2]Cl$[c] (room temp)	solid	0.17(1)	2.03(1)	0.20(1)/0.26(1)	this work
6	$[Fe^{III}TPP(4\text{-}MeIm)_2]Cl$	crystalline	0.34(3)	2.26(3)	0.46(4)/0.96(6)	this work
11/**12**	$[Fe^{III}TMP$[d] $(1\text{-}MeIm)_2]ClO_4$	crystalline	0.28	2.28	0.71/0.94	9
	$[Fe^{III}PPIX(HIm)_2]^+$	dmso	0.22(2)	2.38(2)	0.21(3)/0.26(4)	4
		water/ethanol[d]	0.24(1)	2.35(1)	0.31(1)/0.32(1)	4
		solid	0.24	2.30	not given	17
	$[Fe^{III}PPIX(1\text{-}MeIm)_2]^+$	dmso	0.23(1)	2.24(1)	0.37(1)/0.49(2)	4
		water/ethanol[d]	0.26(1)	2.34(1)	0.16(1)/0.18(1)	4
	$[Fe^{III}PPIX(2\text{-}MeIm)_2]^+$	water/ethanol[d]	0.16(2)	1.87(2)	10.29(1)/0.59(3)	4
	$Fe^{III}PPIX(histidine)_2]^+$	water (pH 10.1)	0.26(6)	1.99(6)	0.19(8)/0.30(9)	3
	$[Fe^{III}PPIX$ $(N^{\alpha}\text{-}histidine)_2]^+$	water/ethanol (pH 8.4)	0.21(3)	2.09(3)	0.40(3)/0.61(6)	3
	$[Fe^{III}PPIX(histamine)_2]+$	water (pH 11.0)	0.28(5)	2.28(5)	0.32(4)/0.42(8)	3
	$\{Fe^{III}PPIX(pilocarpate)]^+$	water (pH 10.1)	0.26(2)	2.22(2)	0.36(2)/0.44(4)	3

[a] Relative to metallic iron at 298 K. [b] Half-width at half-height. [c] Additional site in EPR spectrum. [d] TMP = 5,10,15,20-tetramesitylporphyrinato dianion.

b. Preparation of Bis(4-methylimidazole)tetraphenylporphyrinatoiron(III) (6). The preparation is as for the preparation of the bis(imidazole) complex except that 4-methylimidazole (0.05 g; 0.6 mmol) was used.

Mössbauer Spectroscopic Measurements. Mössbauer spectra were recorded at room temperature or at 77 K. The apparatus and methodology have been described previously.[39]

EPR Spectroscopic Measurements. The apparatus and methodology are as described in our previous paper.[1]

Crystal Structure Determination of 6. A black plate crystal was selected and mounted on the end of a glass fiber. The crystal was transferred to a Rigaku AFC7R four-circle diffractometer equipped with an Oxford Cryosystems cryostream cooler,[40] operating at 123(1) K. Unit cell constants were determined prior to data collection by least-squares refinement of 25 reflections well-positioned throughout reciprocal space, $51.35° \le \theta \le 54.50°$. The data were corrected for Lorentz polarization effects. An analytical absorption correction was applied; maximum and minimum correction factors were 0.734 and 0.234, respectively. The intensity of three standard reflections monitored every 150 reflections showed an overall decrease in the intensity over the period of the data collection of 3.84%, and the data were adjusted accordingly. A total of 10 038 reflections were measured of which 9354 were unique, $R_{int} = 0.0254$. A total of 7719 reflections were observed with $I > 2\sigma(I)$.

The structure of **6** was solved by direct methods (SHELXS-86),[41] with full-matrix least-squares refinement on F2 (SHELXL-94).[42] Non-hydrogen atoms were refined with anisotropic displacement parameters, and hydrogen atoms were included using a riding model. A correction for secondary extinction, $x = 0.00179(14)$, according to the method in SHELXL-97 was included. $S = 1.015$, $w = 1/[\sigma^2(F_o^2) + (0.0722P)^2 + 3.1518P]$ where $P = (F_o^2 + 2F_c^2)/3$. Maximum and mean Δ/σ were 0.001 and 0.000, respectively. Maximum and minimum Δ/ρ were 0.78 and -0.74 e Å^{-3}.

Results and Discussion

EPR Data. The EPR *g*-values for $[Fe^{III}TPP(HIm)_2]Cl$, $[Fe^{III}TPP(4\text{-}MeIm)_2]Cl$, and related $[Fe^{III}Por(L)_2]^+$ complexes[7,11,13−15,19] (where L = imidazole or substituted imidazole) are presented in Table 1. The bis(imidazole complex) was prepared several times. In all three, different EPR signals were observed, i.e., from three different structural forms (two of which are in the triclinic structure reported by Scheidt et al.[5]). Most samples give an EPR spectrum with only one site, which was the overlap of the two sites observed by Strouse et al.[13,19] In one case an additional site was observed. The parameters of this second site were reasonably similar to the *g* values observed for [K(K222)]-$[Fe^{III}TPP(4\text{-}MeIm^-)_2]$,[14] where both the axial ligands were deprotonated. It is extremely doubtful that there was formation of a bis(imidazolato) complex under the conditions used, and in addition a cation would be required to balance the charge. There was no analytical evidence for this. There are two other possible explanations. Either only one axial ligand was deprotonated and that the species that gave rise to the second site is $[Fe^{III}TPP(HIm)(Im^-)]$ (this we believe is still unlikely because the counterion would have to be H^+) or a second $[Fe^{III}TPP(HIm)_2]Cl$ solid was synthesized that had a structure similar to that reported by Hoard et al.[6] We believe this has occurred because the analysis indicated this formulation. We note that others could not prepare this crystalline form. We were only able to prepare it together with the other form and not by itself. The parameters we obtained of solid $[Fe^{III}TPP(4\text{-}MeIm)_2]Cl$ agree with the values presented by Walker, Reis, and Balke[15] for a frozen solution study.

Mössbauer Data. The Mössbauer parameters for the bis(imidazole), bis(4-methylimidazole) derivatives, and similar compounds[3,4,9,17] are presented in Table 2. The parameters for the bis(imidazole) compound for all but one sample were in good agreement with those of Epstein et al.[17] In one case the ΔE_Q value was lower than expected. This was the material that showed the presence of two EPR signals.

Crystal and Molecular Structure of $[Fe^{III}TPP(4\text{-}methylimidazole)]Cl$. The crystal structure of **6** reveals that there are two independent molecules in the unit cell. The single-crystal crystallographic data are reported in Table 3, and a comparison of selected bond lengths and angles in the two molecules is given in Table 4. The coordination around the Fe atom in

(39) Hamed, M. Y.; Hider, R. C.; Silver, J. *Inorg. Chim. Acta* **1982**, *66*, 13−18.
(40) Cosier, J.; Glazer, A. M. *J. Appl. Crystallogr.* **1986**, *19*, 105−107.
(41) Sheldrick, G. M. *Acta Crystallogr.* **1990**, *A46*, 467−473.
(42) Sheldrick, G. M. *FHELXTL*, version 5; Brooker AXF: Madison, WI, 1994.

Table 3. Crystallographic Data for Compound **6**

chemical formula	C54 H42 C17 Fe N8
a, Å	12.0001(14)
b, Å	21.204(4)
c, Å	10.505(2)
α, deg	91.51(2)
β, deg	106.601(12)
γ, deg	88.84(2)
V, Å^3	2560.3(7)
fw	1106.96
space group	$P\bar{1}$
temp, K	123(1)
λ, Å	1.541 78
ρ (calcd), mg/cm^3	1.436
transm coeff	0.234−0.734
R	0.0468
R_w	0.1245

Table 4. Selected Bond Lengths and Angles in Molecules **6a** and **6b**

iron coordination	**6a**	**6b**
	Bond Length (Å)	
Fe−N_{por}	2.008(2)	2.002(2)
Fe−N_{por}	1.993(2)	1.988(2)
Fe−N_{axial}	1.975(2)	1.987(2)
	Bond Angle (deg)	
N_{por}−Fe−N_{por}	89.77(10)	89.76(10)
	90.23(10)	90.24(10)
N_{axial}−Fe−N_{por}	91.91(10)	92.06(9)
	88.09(10)	87.94(9)
	89.71(10)	89.28(10)
	90.29(10)	90.73(10)

molecule **6a** (Figure 2) shows it to be very similar to that of compound **1,** the bond lengths being the same within experimental error and the ϕ angle also similar. Molecule **6b** has a similar ϕ angle but has a slightly longer Fe−N_{axial} distance. However the distances in **6b** are in the range of distances in compounds **1**−**3** and the ϕ angle is close to **1**. Hence, molecules **6a** and **6b** are very similar, and so we might not expect to see two distinct EPR signals, and indeed we do not.

Other than the differences in the length of the Fe−N_{por} bonds in molecules **6a** and **6b** all other distances within the porphyrin ring are very similar. Both porphyrin rings are flat, with the largest deviations from the plane for **6a** being −0.061(2) Å (N1) and for molecule **6b** being +0.077(2) Å for N5. The packing diagram of **6** is shown in Figure 3. There are four $CHCl_3$ molecules (two equivalent pairs) in the unit cell and two equivalent Cl^- ions. The latter are each hydrogen-bonded through one hydrogen of a protonated nitrogen of an imidazole ring to both **6a** and **6b** and to the hydrogen atoms of two different $CHCl_3$ molecules. Thus, each imidazole ring of both molecules **6a** and **6b** bonds to a Cl^- ion via a hydrogen bond. The shortest H bonds are from molecule **6a** to Cl^- (2.125(1) Å), whereas those from **6b** to Cl^- are 2.264(1) Å long. The $CHCl_3$ to Cl^- H bonds are longer at 2.308(1) and 2.549(1) Å, respectively. The presence of the H bonds from the imidazole rings is consistent with the findings in the structures of compounds **1**−**5** and further adds evidence to the possibility of such bonding being a control mechanism of haem iron reactivity in cytochrome *b*[43,44] and other haemproteins.[29]

It is worth noting that the shorter H bonds found in molecule **6a** may explain why the Fe−N_{axial} bonds are also the shortest in this molecule. As the Cl^- pulls the proton toward itself, the latter attracts less negative charge from the imidazole ring. This allows stronger π-bonding (electron donation) from the methyl imidazole ligands to the iron atom in **6a** and hence shorter Fe−N_{ax} bonds. In molecule **6b**, where the H bonds are longer, the imidazole character from H-bonding will be larger (hence, negative charge is increased). This might have been expected to shorten the Fe−N bond on an electrostatic argument. Clearly, this is not observed and indicates that π-bonding rather than σ-bonding is dominant.

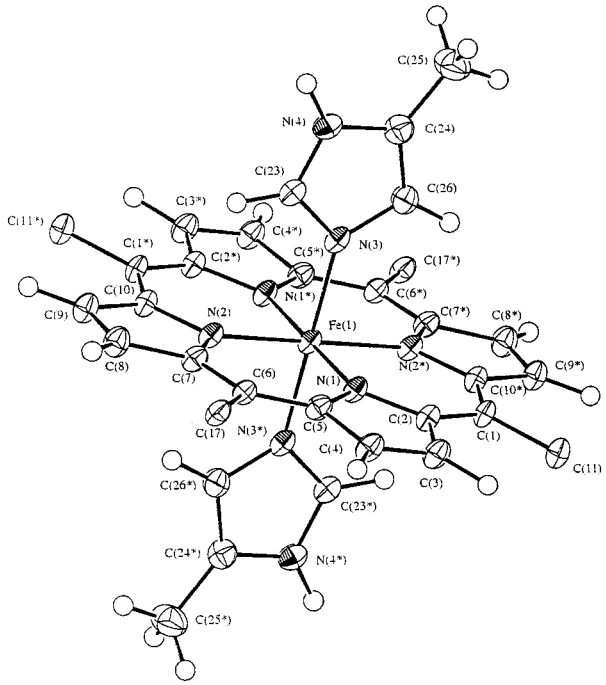

Figure 2. Crystal structure of [Fe^{III}TPP(4-methylimidazole)$_2$]Cl.

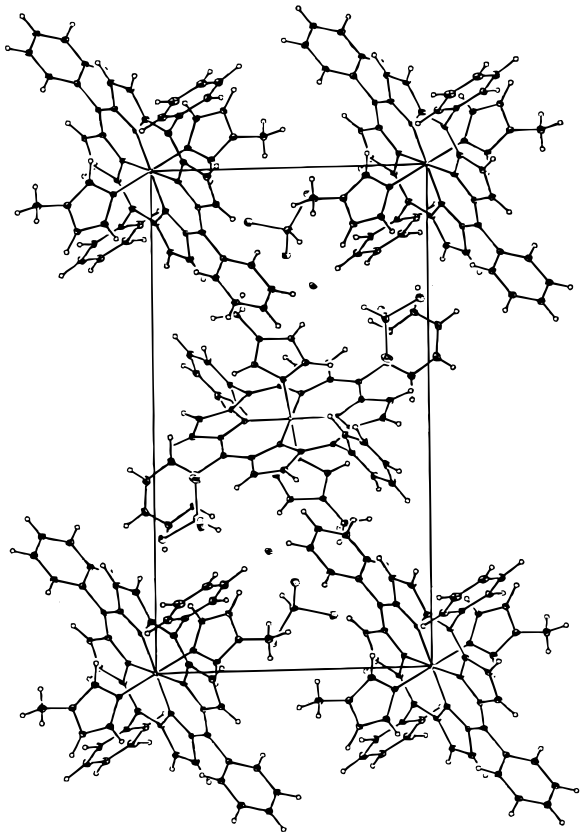

Figure 3. Packing diagram of [Fe^{III}TPP(4-methylimidazole)$_2$]Cl.

(43) Brautigan, D. L.; Feinberg, B. A.; Hoffman, B. M.; Margoliash, E.; Peisach, J.; Blumberg, W. E. *J. Biol. Chem.* **1977**, *252*, 574−582.
(44) De Ropp, J. S.; Thanabal, V.; La Mar, G. N. *J. Am. Chem. Soc.* **1985**, *107*, 8268−8270.

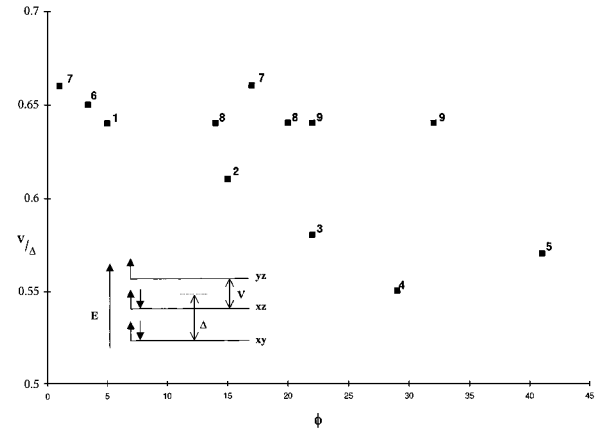

Figure 4. Plot of ϕ vs $^{V}/\Delta$.

Effects of Orientation of the Axial Ligands. It has been shown that when the electron configuration of low-spin Fe(III) is $(d_{xy})^2(d_{xz},d_{yz})^3$ even for metalloporphyrins that are equatorially symmetrical and have perpendicular bound identical axial ligands, then the iron is in a rhombically distorted system.[9,45] The electronic structure of these complexes may be described in terms of the crystal field parameters V and Δ where V is the rhombic splitting parameter and Δ is the tetragonal splitting parameter (Figure 4). The wave functions are linear combinations of the three states with coefficients a (for d_{yz}), b (for d_{xz}), and c (for d_{xy}). The $d_{x^2-y^2}$ and d_{z^2} are considered to be of too high energy to contribute. By use of the axis system of Taylor,[45] it has been shown[9] that

$$g_x = 2[a^2 - (b + c)^2], \quad g_y = 2[(a + c)^2 - b^2], \quad g_z = 2[(a + b)^2 - c^2]$$

and the crystal field parameters $^{V}/_{\lambda}$ and $^{\Delta}/_{\lambda}$ may be described as

$$^{V}/_{\lambda} = E_{yz} - E_{xz} \quad \text{and} \quad ^{\Delta}/_{\lambda} = E_{yz} - E_{xy} - (^{1}/_{2})(^{V}/_{\lambda})$$

Therefore, $^{V}/_{\lambda} = g_x/(g_z + g_y) + g_y/(g_z - g_x)$ and $^{\Delta}/_{\lambda} = g_x/(g_z + g_y) + g_z(g_y - g_x) - (^{1}/_{2})(^{V}/_{\lambda})$. Strouse and co-workers[13,19] proposed that $^{V}/_{\Delta}$, readily derived from EPR parameters,[45] could be related to ϕ. Scheidt et al.[11] calculated $^{V}/_{\Delta} = 0.635$ for complex **9**. This agreed poorly with the correlation of Strouse and co-workers,[13,19] who predicted a value of $^{V}/_{\Delta} = 0.58-0.54$ for $\phi = 22-32°$. Scheidt et al.[11] suggested that the poor agreement might be due to two possible reasons. First, the correlation was derived from complexes **1**−**5** that have parallel imidazole planes, whereas there is an angle between the ligand planes of complexes **7**−**9**. These compounds give $^{V}/_{\Delta}$ values that do not agree with the correlation (Figure 4). Second, the correlation was derived for imidazole derivatives unsubstituted at the 1-position and may not be expected to work for other derivatives, especially as Walker, Lo, and Ree[46] have described pK_a versus ligand binding equilibrium constant relationships for imidazole derivatives substituted at the 1-position and unsubstituted derivatives. The values for the two types are significantly different. This latter reason is certainly wrong because complex **7** has ligands that are not substituted in the 1-position and is related to complex **6**.

Our complex (**6**) does follow the original trend, and the angle between the ligand planes ($\Delta\phi$) is near zero. It therefore appears that the trend is a significant finding. The fact that the correlation breaks down for $\Delta\phi$ angles greater than zero suggests that metal−ligand bonding involves t_{2g} orbitals, which make an important contribution to the EPR parameters.

It is obvious that for parallel planes bonding of both ligands to the singly occupied d orbital is important. This will be smaller if the $\Delta\phi$ angle is larger than zero. An examination of the bond lengths in Table 5 for compounds **1**−**6** is instructive. As ϕ increases, the difference between the long and short Fe−N_{por} bonds diminishes. Compounds **1**, **2**, and **6** (which have smaller ϕ values) have larger differences between the long and short Fe−N_{por} bonds than compounds **3**−**5**. In all the compounds **1**−**6** the Fe−N_{ax} bond lengths are shorter than the Fe−N_{por}. The bond lengths suggest that the strongest bonding is in the axial direction in **1**−**6**. This most probably results from strong π-bonding from the axial ligands, whereas the porphyrin π-bonding to the iron t_{2g} orbitals is manifestly weaker. This would agree with previous Mössbauer spectroscopic measurements on the sign of the field gradient that suggests that the highest electron population lies in the axial direction.[47]

For compounds **8** and **9**, which do not fit the curve in Figure 4, the situation is very different. The Fe−N_{por} bonds are overall noticeably shorter than in compounds **1**−**6**, showing stronger bonding between the porphyrin and the iron atom; in addition the axial bonding distances are more equal in length to the Fe−N_{por} distances. The extent that this is caused by or in fact causes the $\Delta\phi$ angle cannot be deduced. Compound **7**, which also does not fit the relationship in Figure 4, has a much less accurately known structure that limits the validity of any deductions. The Fe−N_{por} distances are long, but the errors could bring them in line with compounds **8** and **9**. However, the axial bonds are very short, even allowing for the errors. This would be expected for strong ligand π-bonding to the iron. In this case the ligands are very electron-rich, having electron donors on the second nitrogen atom rather than a hydrogen atom. We will discuss this point further in the next section of the paper.

There are no EPR measurements in the literature for compounds **10**−**12**. Compounds **10** and **11** have similar structural features to compounds **8** and **9**, whereas compound **12** is very similar to compounds **4** and **5**. Compound **13** is very likely to be responsible for the second EPR site we recorded when we prepared the material of this formula. This compound would then have a g_z of 2.673 and a $^{V}/_{\Delta}$ of 0.76. Clearly, this does not fit the correlation in Figure 4, but if the axial bond lengths are averaged, then it is similar to compounds **8**−**10**.

Is the correlation useful? Only if it is assumed that a compound or haem protein of unknown structure has a $\Delta\phi$ value of zero can an EPR g_z value be translated into a ϕ angle. However, it could be argued that this is of limited value because the only way (to date) to measure $\Delta\phi$ is a structural analysis, which of course would also give ϕ. For cases where EPR spectra change with pH as in cytochrome b_5[47] or where they differ for the low- and high-potential forms as in chloroplast cytochrome b_{559},[24] using the correlation and assuming $\Delta\phi$ is 0 may aid the understanding of the role of the haem. Of course, the EPR spectra must be of the rhombic type before this correlation is applied.

It should be noted that the compounds that do not fit the correlation (**8** and **9**) are substituted in the 1-position (Figure 1) and that compound **7** carries a negative charge that will be predominantly focused at the 1-position. The 1-position is not substituted in histidine residues bonding in haemproteins, and

(45) Taylor, C. P. S. *Biochim. Biophys. Acta*. **1977**, *491*, 137−149.
(46) Walker, F. A.; Lo, M. W.; Ree, M. T. *J. Am. Chem. Soc.* **1976**, *98*, 5553−5560.
(47) Peisach, J.; Mims, W. B. *Biochemistry* **1977**, *16*, 2795−2799.

Table 5. Comparison of Major Bond Lengths and Angles around the Iron Atoms and g_z Values Where Known

	complex	g_z	Fe−N_{por} (Å)		Fe−N_{ax} (Å)	ϕ (deg)	$\Delta\phi$ (deg)	ref
7	[K(K222)]	2.6	2.031(12)	1.974(11)	1.958(12)	1	18	14
	[Fe^{III}TPP(4-MeIm)$_2$]		2.006(12)	1.982(11)	1.928(12)	17		
6a	[Fe^{III}TPP(4-MeIm)$_2$]Cl	2.859	2.008(2)	1.993(2)	1.975(2)	3.1(1)	0	this work
6b	[Fe^{III}TPP(4-MeIm)$_2$]Cl	2.859	2.002(2)	1.988(2)	1.987(2)	4.6(2)		
9	[Fe^{III}TPP	2.866	1.988(3)	1.969(3)	1.970(3)	22	10	11
	(1-MeIm)$_2$]ClO_4		1.993(3)	1.977(3)	1.978(3)	32		
8	[Fe^{III}T2,6-Cl_2PP	2.9	1.988(4)	1.971(4)	1.976(4)	14	6	7
	(1-VinIm)$_2$]ClO_4		1.981(4)	1.973(4)	1.968(4)	20		
1	[Fe^{III}TPP(HIm)$_2$]Cl.	2.916	2.002(3)	1.985(3)	1.977(3)	5	0	5, 19
3	[Fe^{III}TPP(*t*-MU)$_2$]SbF_6	2.964	1.995(4)	1.988(4)	1.983(4)	22	0	13
2	[Fe^{III}TPP(*c*-MU)$_2$]SbF_6	2.965	2.007(6)	1.983(7)	1.979(7)	15	0	13
5	[Fe^{III}TPP(HIm)$_2$]Cl.	2.988	1.995(3)	1.990(3)	1.964(3)	41	0	5, 19
4	[Fe^{III}TPP(*c*-MU)$_2$]SbF_6	2.999	1.998(7)	1.996(7)	1.967(7)	29	0	13
10	[Fe^{III}PPIX		2.012(5)	1.973(6)	1.988(5)	3	13	16
	(1-MeIm)$_2$]ClO_4		1.992(5)	1.985(5)	1.966(5)	16		
11	[Fe^{III}TMP	*a*	2.002(3)	1.974(2)	1.975(3)	23	0	9
	(1-MeIm)$_2$]ClO_4							
12	[Fe^{III}TMP	*a*	2.005(3)	1.999(3)	1.965(3)	36	0	9
	(1-MeIm)$_2$]ClO_4							
13	[Fe^{III}TPP(HIm)$_2$]Cl		1.987(4)	1.990(4)	1.991(5)	18	57	6
			1.999(4)	1.980(4)	1.957(4)	39		
14	[Fe^{III}TPP	3.70	1.988(5)	1.986(5)	2.005(5)	34	86	58
	(Py)$_2$]ClO_4		1.982(4)	1.972(5)	2.001(5)	38		
15	[Fe^{III}TPP	3.56[b]	1.976(4)	1.966(4)	2.015(4)	32	89	20
	(2-MeIm)$_2$]ClO_4		1.968(4)	1.972(4)	2.010(4)	32		
16	[Fe^{III}TMP	3.07	1.968(7)	1.969(7)	2.018(7)	29	77	59
	(3-ClPy)$_2$]ClO_4		1.971(7)	1.964(7)	2.006(7)	48		
17	[Fe^{III}TMP	2.53	1.957(5)	1.955(6)	2.021(6)	43	90	47
	(4-CNPy)$_2$]ClO_4		1.971(5)	1.959(6)	2.001(5)	44		
18	[Fe^{III}TMP	2.89	1.966(3)	1.958(4)	2.002(4)	44	90	59
	(3-EtPy)$_2$]ClO_4		1.968(3)	1.962(4)	1.989(4)	44		
19	[Fe^{III}TMP	3.48	1.969(4)	1.950(4)	1.989(4)	37	79	9
	(4-Me_2NPy)$_2$]ClO_4		1.966(4)	1.973(4)	1.978(4)	42		
20	[Fe^{III}TPP	2.54	1.950(4)	1.944(4)	2.008(4)	36	89	60
	(4-CNPy)$_2$]ClO_4		1.957(4)	1.958(4)	1.997(4)	35		
21	[Fe^{III}OEP((C_5H_5)	3.24	2.023(4)	2.004(4)	2.057(5)	23	0	57
	(C_4NH_4)Fe)$_2$]O_3SCF_3							
22	[Fe^{III}OEP	2.818	1.987(2)	1.986(2)	1.995(2)	41	0	9
	(4-NMe_2Py)$_2$]ClO4							
23	[Fe^{III}OEP		1.999(2)	1.990(2)	2.031(2)	41	0	61
	(3-Clpy)$_2$]ClO_4							

[a] Solid-state data were too complex to fit but are said to be the rhombic type (ref 9). [b] Reference 8.

thus, the fact that compounds **7**−**9** do not fit the correlation does not negate its use because it could be argued that they are not relevant. If this is the case, then all the relevant compounds (**1**−**6**) fit the correlation and in all cases $\Delta\phi$ equals 0. Therefore, we would expect that in haemproteins (containing two histidines) $\Delta\phi$ would equal zero (if the EPR spectra were rhombic) and the correlation can be applied.

It is useful to see to what extent this is true. A number of crystal structures of cytochromes b_5 and cytochromes bc_1 complexes have been solved to varying degrees of resolution. Of the three known X-ray structures of cytochromes b_5, all show that the histidine ligands to the *b* haems are very close to parallel, with $\Delta\phi$ angles close to or equal to zero (allowing for the resolution of the structures).[48−50] Moreover, the ϕ values are close to 40°. This value is similar to that expected from the $^{\Delta}/_{\lambda}$ value for neutral cytochrome b_5 of 0.52.[35,36,47,51] In addition, a cytochrome b_5 structure derived from solution NMR studies[52] also shows a $\Delta\phi$ angle close to parallel and a ϕ value of ∼40°.

There have been a number of reports of the crystal structures of cytochromes bc_1.[53−56] The cytochrome *b* haems in these structures have $\Delta\phi$ close to or equal to 90° and ϕ angles around 40−45°. The EPR spectra of these *b* haems are of the "large g_{max}" type,[13] typical of iron porphyrin complexes where the imidazole rings of the axial ligands are perpendicular to one another, and so of course, we would not expect them to obey the correlation in Figure 4.

It is clear that compounds **14**−**20**, which are "large g_{max}" class, all have much smaller Fe−N_{por} distances arising from strong iron t_{2g} π-bonding to the N_{por} orbitals and long bonds to the axial ligands. This suggests in all these cases (compounds **14**−**20**), with the possible exception of compound **19**, that the iron to N_{ax} π-bonding is very weak or does not exist at all, which is in agreement with our previous findings.[1]

(48) Matthews, F. S.; Argos, P.; Levine, M. *Cold Spring Harbor Symp. Quant. Biol.* **1971**, *36*, 387.
(49) Rodriguez-Maranon, M. J.; Qiu, F.; Stark, R. E.; White, S. P.; Zhang, X.; Foundling, S. I.; Rodriguez, V.; Schilling, C. L.; Bunce, R. A.; Rivera, M. *Biochemistry* **1996**, *35*, 16378−16390.
(50) Rivera, M.; Seetharaman, R.; Girdhar, D.; Wirtz, M.; Zhang, X.; Wang, X.; White, S. *Biochemistry* **1998**, *37*, 1485−1494.
(51) Guzov, V. M.; Houston, H. L.; Muratalier, M. B.; Walker, F. A.; Feyeriesen, R. *J. Biol. Chem.* **1996**, *271*, 26637−26645.
(52) Arnesano, F.; Banci, L.; Bertini, I.; Felli, I. C. *Biochemistry* **1998**, *37*, 173−184.
(53) Zhang, Z.; Huang, L.; Shulmeister, V. M.; Chi, Y. I.; Kim, K. K.; Hung, L.; Crofts, A. R.; Berry, E. A.; Kim, S. H. *Nature* **1998**, *392*, 677−684.
(54) Xia, D.; Yu, C. A.; Kim, H.; Xia, J. Z.; Kachurin, A. M.; Zhang, L.; Yu, L.; Deisenhofer, J. *Science* **1997**, *277*, 60−66.
(55) Iwata, S.; Lee, J. W.; Okada, K.; Lee, J. K.; Iwata, M.; Rasmussen, B.; Link, T. A.; Ramasawamy, S.; Jap, B. K. *Science* **1998**, *281*, 64−71.
(56) Crofts, A. R.; Hong, S. J.; Ugulava, N.; Baraquera, B.; Gennis, R.; Geurgova-Kuras, M.; Berry, E. A. *Proc. Natl. Acad. Sci. U.S.A.* **1999**, *96*, 10021−10026.

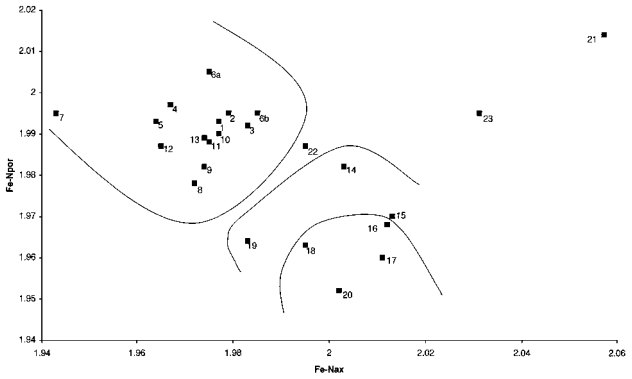

Figure 5. Plot of average $Fe-N_{por}$ distance vs average $Fe-N_{ax}$ distance.

Simple Explanation of the Different Ground States. The plot of average $Fe-N_{por}$ distance (average of all four Fe−N porphyrin distances) against $Fe-N_{ax}$ distance (Figure 5) is instructive. The compounds on the plot can be divided into four groups except for compound **21**[57] (which is discussed below). Compounds **1**−**13** and **22**[5−7,9,11,13,14,16,19] have all been shown to have a $(d_{xy})^2(d_{xz},d_{yz})^3$ ground state, which is an orbital singlet (^{2}B), and the unpaired electron is localized in the d_{yz} orbital.[1,57] Of these compounds, **1**−**13** are within the same area (presented with an arbitrary oval line) of the plot. Two other areas are also shown on the plot. In the area between the smaller and larger areas are compounds **14**, **15**, and **19**.[9,20,58] These are the "large g_{max}" class and have an orbital doublet (^{2}E) ground state. Thus, from this plot the different ground states can be simply explained in terms of crystal field effects of the six ligand atoms (the nitrogen atoms) nearest the iron. When the axial ligands are sterically hindered, then they are more weakly bonded than the porphyrin nitrogen ligands and the $(d_{xz},d_{yz})^4(d_{xy})^1$ ground state is preferred. Such compounds are **16**−**18** and **20**[9,59,60] shown within the smaller arc. For compounds in the latter two cases the axial ligands are perpendicular and the $Fe-N_{ax}$ bond lengths differ (their average is plotted) in Figure 5.

The perpendicular arrangement arises for the $(d_{xy})^2(d_{xz},d_{yz})^3$ ground state either from an electronic interaction of the Fe $(d_{xy})^2$ orbital and the axial ligand π-orbitals, though donation from the latter to the former would be very weak, or more likely through $d_\pi-p_\pi$ weak bonding interactions from the iron d_{xz} or d_{yz} orbitals donating each to different axial ligands. For the $(d_{xz},d_{yz})^4(d_{xy})^1$ case the perpendicular arrangement is probably due to interactions with the filled iron d_{xz} and d_{yz} orbitals and the axial ligands.

The EPR results fit clearly into two distinct types, both relating to low-spin Fe(III) complexes. One set fits nicely onto the correlating graph shown in ref 1. There are always three well-defined features, g_y falling close to 2.2 while g_x and g_z vary together, with g_z decreasing as g_x increases. These range from ca. 1.95 to 1.5 for g_x and ca. 2.5 to 3.0 for g_z. All these compounds are on the left of the plot in Figure 5.

The other set (compounds **14**−**20** on the right-hand side of the plot in Figure 5) is quite different, the key difference being the very large high-field shifts for g_z ($g_{||}$), together with major line broadening of features in this region, and no other feature. This clear difference between the structures fits well with the two kinds of geometry. The first arises from the ^{2}B ground state. The second, when nonsterically hindered, arises from the ^{2}E ground state and when sterically hindered from the $(d_{xz},d_{yz})^4(d_{xy})^1$ ground state.

Compound **21**, which we recently reported,[57] is unusual. It has the longest axial Fe−N bond lengths (sterically hindered) and has a rhombic type EPR spectrum but with its g_z value near those found for "large g_{max}" type EPR spectra. Thus, it has the $(d_{xy})^2(d_{xz},d_{yz})^3$ ground state. As can be seen from Figure 5, it is no closer to the 45° line (ideal octahedral structure) than the other compounds. The axial azaferrocene ligands in this compound are poor π-acceptors but good σ-donors. These axial ligands are sterically hindered from approaching the Fe atom, though like the imidazoles, they are five-membered rings and so might otherwise have been expected to get closer to the iron atom. The large "g_{max}" compound closest to **21** is compound **14**. Compound **14** is a pyridine complex of tetraphenylporphyrinatoiron(III). It is worth noting that the $[FePPIX(py)_2]^+$ complex has in fact a $(d_{xy})^2(d_{xz},d_{yz})^3$ ground state.[9,17] The latter porphyrin, unlike TPP, has no bulky side groups to interact sterically with the pyridine, and so the pyridine N atom can bind more strongly. Compounds **22** and **23**[61] are the closest compounds to compound **21**. They are also Fe^{III}OEP complexes. Here, the iron−nitrogen porphyrin bond lengths are shorter than compound **21** even though the axial ligands are weak, supporting the fact that the ligands in compound **21** are sterically hindered. Compounds **22** and **23** are known to have a $(d_{xy})^2(d_{xz},\ d_{yz})^3$ ground state.[62−64]

It thus appears that Figure 5 may be useful in considering which axial ligands would control the ground state of the iron for a given porphyrin. For instance, it may be possible to choose an axial ligand that would change its ground state with an iron porphyrin as a function of temperature. $[Fe^{III}OEP(4\text{-}NMe_2Py)_2]ClO_4$, compound **22**, has been shown to exist in two forms, one of which is said to exist in a high- and low-spin equilibrium.[9,62] Moreover, a range of Fe^{III}OEP-substituted bispyridine compounds have been shown to exhibit such behavior.[63,64] It is significant that it is the Fe^{III}OEP compounds that lie between the ^{2}B and ^{2}E ground states. Compounds **21** and **22** may lie near the true boundary between ^{2}B and ^{2}E states, where an intermediate spin complex has been reported.[59]

This explanation of the different ground states also gives further insight into the compounds that obey the relationship between V and Δ. For the imidazole ligands in Figure 5 it is apparent that compounds **1**−**6** (which have the relationship shown in Figure 4) all have a large $Fe-N_{por}$ average distance (greater than 1.99 Å). Of the other compounds with imidazoles as axial ligands (that have known EPR spectra), only compound **7** has such a value. This compound is very electron-rich and is a good π-donor. For one of the two axial ligands, $\phi = 1°$ and the ligand is thus very suitable for π-bonding to the half-occupied iron orbital and does this very well, and the other is not too far away, $\phi = 17°$, and cannot donate more density because the iron is probably saturated. Hence, compound **7** does

(57) Cesario, M.; Giannotti, C.; Guilhem, J.; Silver, J.; Zakrzewski, J. *J. Chem. Soc., Dalton Trans.* **1997**, 47−53.
(58) Inniss, D.; Soltis, S. M.; Strouse, C. E. *J. Am. Chem. Soc.* **1988**, *110*, 5644−5650.
(59) Safo, M. K.; Gupta, G. P.; Watson, C. T.; Simonis, U.; Walker, F. A.; Scheidt, W. R. *J. Am. Chem. Soc.* **1992**, *114*, 7066−7075.
(60) Safo, M. K.; Walker, F. A.; Raitsimring, A. M.; Walters, W. P.; Dolata, D. P.; Debrunner, P. G.; Scheidt, W. R. *J. Am. Chem. Soc.* **1994**, *116*, 7760−7770.
(61) Scheidt, W. R.; Geiger, D. K.; Haller, K. J. *J. Am. Chem. Soc.* **1982**, *104*, 495−499.
(62) Scheidt, W. R.; Geiger, D. K.; Hayes, R. G.; Lang, G. *J. Am. Chem. Soc.* **1983**, *105*, 2625−2632.
(63) Hill, H. A. O.; Skyte, P. D.; Buchler, J. W.; Lueken, H.; Tonn, M.; Gregson, A. K.; Pellizer, G. *J. Chem. Soc., Chem. Commun.* **1979**, 151.
(64) Gregson, A. K. *Inorg. Chem.* **1981**, *20*, 81−87.

in fact fit the relationship in Figure 5 rather well if the angle of the second axial ligand is neglected.

Because the relationship in Figure 4 therefore appears significant, it may be possible to read off a ϕ angle for a measured value of $^{V}/_{\Delta}$. For instance, cytochrome b_5 has $^{V}/_{\Delta} = 0.52$ in neutral solution and a value of 0.66 in alkaline media.[47] From Figure 4 this may mean that the ϕ angle of the "parallel" ligand planes changes from 35° to about 0° as the solution is made alkaline. Similarly, cytochrome b_{559}[24] may have an angle around 25° in the low-potential form and a very different angle where $^{V}/_{\Delta} = 0.41$ in the high-potential form.

At first sight it may be thought that this ignores effects such as imidazolate character (which may be important in the experiment that is in alkaline media), tilt distortion, changes in degree of tetragonality or in ruffling. However, all these physical properties will have affected the compounds in the correlation, and yet the correlation holds. So it is reasonable to assume that they are minor effects and that the dominant effect is the ϕ angle and $^{V}/_{\Delta}$ value (though the correlation to some extent may be based on a small contribution to these factors).

Conclusions

We have been able to demonstrate two findings for $[Fe^{III}Por(L)_2]^+$ complexes.

1. There is a simple plot of average $Fe-N_{por}$ distance against average $Fe-N_{ax}$ distance that rationalizes the underlying difference in the low-spin Fe^{III} ground states. Further, this plot may be used to forecast which axial ligands control which ground state and what type of properties need to be designed into a ligand to approach these boundary conditions.

2. A previously reported correlation is significant and may be used to forecast the angles between parallel imidazole planes and the $Fe-N_{por}$ vector (the ϕ angles) in proteins if the EPR spectra are known. It has been shown that complex **6**, $[Fe^{III}TPP(4\text{-}MeIm)_2]Cl$, which has parallel imidazole planes, fits the correlation shown Figure 4.

The angle between the planes of the ligands is clearly important for complexes **7**−**9** that do not fit the correlation well. The ligands of complexes **7** and **9** can be thought of as being electron-rich and so would be good electron donors through the nitrogen atom lone pair. 1-Vinylimidazole, the ligand of complex **8**, might be expected to be electron-poor if the vinyl group is electron-withdrawing. Thus, the reasons for these complexes having nonparallel ligand planes are obviously complicated.

IC990848S